Molecular Plant Pathology

MOLECULAR PLANT PATHOLOGY (2016) 17(3), 317–329 DOI: 10.1111/mpp.12282

Citrus psorosis virus 24K protein interacts with citrus miRNA precursors, affects their processing and subsequent miRNA accumulation and target expression

CARINA A. REYES[1,*], ELIANA E. OCOLOTOBICHE[1], FACUNDO E. MARMISOLLÉ[1], GABRIEL ROBLES LUNA[1], MARÍA B. BORNIEGO[1], ARIEL A. BAZZINI[2,†], SEBASTIAN ASURMENDI[2] AND MARÍA L. GARCÍA[1]

[1]*Instituto de Biotecnología y Biología Molecular, CCT-La Plata, CONICET—UNLP, Calles 47 y 115, 1900 La Plata, Buenos Aires, Argentina*
[2]*Instituto de Biotecnología, CICVyA-INTA, Hurlingham, Buenos Aires, Argentina*

SUMMARY

Sweet orange (*Citrus sinensis*), one of the most important fruit crops worldwide, may suffer from disease symptoms induced by virus infections, thus resulting in dramatic economic losses. Here, we show that the infection of sweet orange plants with two isolates of *Citrus psorosis virus* (CPsV) expressing different symptomatology alters the accumulation of a set of endogenous microRNAs (miRNAs). Within these miRNAs, miR156, miR167 and miR171 were the most down-regulated, with almost a three-fold reduction in infected samples. This down-regulation led to a concomitant up-regulation of some of their targets, such as *Squamosa promoter-binding protein-like 9* and *13*, as well as *Scarecrow-like 6*. The processing of miRNA precursors, pre-miR156 and pre-miR171, in sweet orange seems to be affected by the virus. For instance, virus infection increases the level of unprocessed precursors, which is accompanied by a concomitant decrease in mature species accumulation. miR156*a* primary transcript accumulation remained unaltered, thus strongly suggesting a processing deregulation for this transcript. The co-immunoprecipitation of viral 24K protein with pre-miR156*a* or pre-miR171*a* suggests that the alteration in the processing of these precursors might be caused by a direct or indirect interaction with this particular viral protein. This result is also consistent with the nuclear localization of both miRNA precursors and the CPsV 24K protein. This study contributes to the understanding of the manner in which a virus can alter host regulatory mechanisms, particularly miRNA biogenesis and target expression.

Keywords: *Citrus psorosis virus*, microRNA processing, *Ophiovirus*, sweet orange.

**Correspondence*: Email: carinar@biol.unlp.edu.ar
†*Present address*: Department of Genetics, Yale University School of Medicine, New Haven, CT 06510, USA.

INTRODUCTION

MicroRNAs (miRNAs) are small RNA molecules that regulate gene expression in plants and animals (Bartel, 2004; Jones-Rhoades *et al*., 2006). Plant primary miRNAs (pri-miRNAs) are synthesized by RNA pol II and have a characteristic 5'cap and 3'poly-A tail (Lee *et al*., 2004; Xie *et al*., 2005). These pri-miRNA transcripts form hairpin-like structures and are sequentially processed by RNAse III-like proteins, namely DICER-like 1 (DCL1) in *Arabidopsis thaliana*, to generate miRNA precursors (pre-miRNAs) and, ultimately, miRNA/miRNA* duplexes (Kurihara and Watanabe, 2004; Park *et al*., 2002). miRNA processing occurs in the specialized D-bodies located in plant nuclei (Fang and Spector, 2007; Fujioka *et al*., 2007; Song *et al*., 2007); DCL1 interacts with the double-stranded RNA (dsRNA)-binding protein HYPONASTIC LEAVES 1 (HYL1) (Han *et al*., 2004; Vazquez *et al*., 2004). In addition, SERRATE and components of the cap-binding complex, which are required for splicing, also contribute to miRNA biogenesis (Gregory *et al*., 2008; Lobbes *et al*., 2006).

A systematic analysis of the mechanism of plant miRNA precursor processing revealed two main models: one progressing base to loop and the other loop to base. The first model implies the recognition of a lower stem (~15 nucleotide) to position for the initial DCL1 cleavage event (Mateos *et al*., 2010). In the second model, the first cut would progress next to the main loop (Bologna *et al*., 2009, 2013a, b). Subsequently, the mature duplex miRNA is exported to the cytoplasm by HASTY (Park *et al*., 2005) and one of the strands is integrated into the RNA-induced silencing complex (RISC), which guides this complex to the complementary mRNA targets. RISC eventually inhibits translation elongation (Brodersen *et al*., 2008) or triggers the degradation of target mRNA (Llave *et al*., 2002).

Several miRNA families are fundamental gene regulatory players in the fine tuning of correct plant development (Schwab *et al*., 2005). In addition, miRNAs also have important functions in the response to biotic stress. For example, *A. thaliana* miR393 is induced by *flg22* (a 22-amino-acid sequence of the conserved N-terminal part of flagellin), thus playing an important role in

plant antibacterial resistance (Navarro *et al*., 2006). Both plant and animal viruses can interfere with miRNA-mediated regulation in the host through different mechanisms exerted at transcriptional or post-transcriptional levels (Cazalla *et al*., 2010; Chapman *et al*., 2004; Chen *et al*., 2004; Kasschau *et al*., 2003; Pfeffer and Voinnet, 2006; Silhavy and Burgyan, 2004). The latter option involves miRNA processing alteration, accumulation and activity.

Originally, most studies have focused on post-transcriptional mechanisms in which increased miRNA levels are associated with the presence of viral suppressors of RNA silencing (VSRs) (Chapman *et al*., 2004; Chen *et al*., 2004; Dunoyer *et al*., 2004; Lakatos *et al*., 2006; Silhavy and Burgyan, 2004). However, other reports have shown that a virus infection and/or the transgenic expression of viral proteins with weak VSR activity can also interfere with miRNA pathways (Bazzini *et al*., 2007; Tagami *et al*., 2007). Indeed, infections by *Tobacco mosaic virus* (TMV) and *Oilseed rape mosaic virus* (ORMV) are clear examples of miRNA alterations at the transcriptional level (Bazzini *et al*., 2009). In addition, the level of conserved miRNAs is reduced after virus infection in tomato, soybean, grapevine and citrus through an alternative molecular mechanism of miRNA interference that cannot be explained by VSR activity (Amin *et al*., 2011; Naqvi *et al*., 2010; Ruiz-Ruiz *et al*., 2011; Singh *et al*., 2012; Yin *et al*., 2013). There are a few examples of viruses interfering with pre-miRNA nuclear export and processing by DICER, as is the case for adenoviruses (Lu and Cullen, 2004). By contrast, to date, there have been no reports of plant viruses interfering with miRNA processing.

Sweet orange (*Citrus sinensis*) is one of the most important fruit crops worldwide. Despite the important roles of miRNAs in plant development, their expression profile and function in non-model plants have been poorly studied and there are few reports on miRNAs in fruit crops (Moxon *et al*., 2008; Song *et al*., 2010a, b; Wang *et al*., 2012; Xu *et al*., 2010, 2013; Zhu *et al*., 2012). The sequence and pattern of about 40 conserved and 10 novel miRNAs were first described in *Citrus reticulata*, *Poncirus trifoliate*, *Citrus clementina* and *Citrus sinensis* using deep sequencing (Song *et al*., 2010a, b). Recently, 227 known miRNAs have been identified in *C. sinensis* (Xu *et al*., 2010, 2013).

Citrus psorosis is a severe viral disease affecting most citrus species. This disease was epidemic in the 1980s and is still present in Argentina and Uruguay (Anderson, 2000; Zanek *et al*., 2006). In the field, symptoms include bark scaling of the trunk on sweet orange, mandarin and grapefruit, as well as chlorotic flecks and spots on young leaves, and a shock reaction expressed as the necrosis of young shoots. The causal agent of the disease is *Citrus psorosis virus* (CPsV), the type member of the genus *Ophiovirus*, family *Ophioviridae* (Garcia *et al*., 1994; Milne *et al*., 2003). CPsV is a tripartite virus with a genome of three single-stranded RNAs (ssRNAs) of negative polarity. RNA 1 codes for the 24K protein and, separated by an intergenic region, the RNA-dependent RNA polymerase (Naum-Ongania *et al*., 2003). RNA 2 harbours the movement protein (54K protein) (Robles Luna *et al*., 2013), whereas RNA 3 codes for the coat protein (Sánchez de la Torre *et al*., 1998). To date, no study has characterized the viral suppressor activity of ophioviruses, and therefore the ability of CPsV to modify miRNA pathways remains completely unknown.

In the present study, we analysed the accumulation of several conserved mature miRNAs, miRNA processing products and their targets in citrus plants infected with two distantly related CPsV isolates that induce symptoms of different severity. We determined that the processing of miR156 and miR171 precursors is affected by CPsV infection in *C. sinensis* plants. The co-immunoprecipitation of 24K viral protein with miRNA precursors in *Nicotiana benthamiana* plants suggests that CPsV directly or indirectly interferes with this mechanism and, consequently, with miRNA and miRNA target accumulation.

RESULTS

Misregulation of conserved citrus miRNAs by CPsV infection

Plant viruses can alter host miRNA and miRNA target expression, including genes involved in plant development and stress responses. To analyse whether CPsV infection modifies miRNA accumulation in citrus and whether there is any association with different symptoms, we infected sweet orange seedlings with the Argentine isolate CPsV 90-1-1 or the distantly related isolate CPV4 from Texas, USA (85% nucleotide identity; Martin *et al*., 2006). The foliar symptoms of CPsV 90-1-1 observed in experimentally graft-inoculated plants include chlorotic flecks and spots on young leaves, as well as wilting and necrosis in young shoots, resulting in a progressive shock reaction (Fig. 1A–C, F). CPV4 shares foliar symptoms with CPsV 90-1-1, but does not produce the shock reaction. Bazzini *et al*. (2007) have previously tested a group of conserved miRNAs, and demonstrated a correlation between symptom severity and alteration in miRNA levels in infected *Nicotiana tabacum* plants. In the present study, 10 conserved miRNAs, including some of those studied by Bazzini *et al*. (2007), were selected and analysed by Northern blot using probes against *Citrus trifoliata* or *Citrus sinensis* miRNA sequences available in miRBase (Table S1, see Supporting Information).

Samples were collected from plants infected with each isolate expressing each characteristic symptom (shock or flecking; Fig. 1A, D, respectively). Virus levels in the different samples were similar (Table S2, see Supporting Information). In parallel, samples were collected from healthy plants with the same shoot size, age and at the same developmental state (Fig. 1E). For the

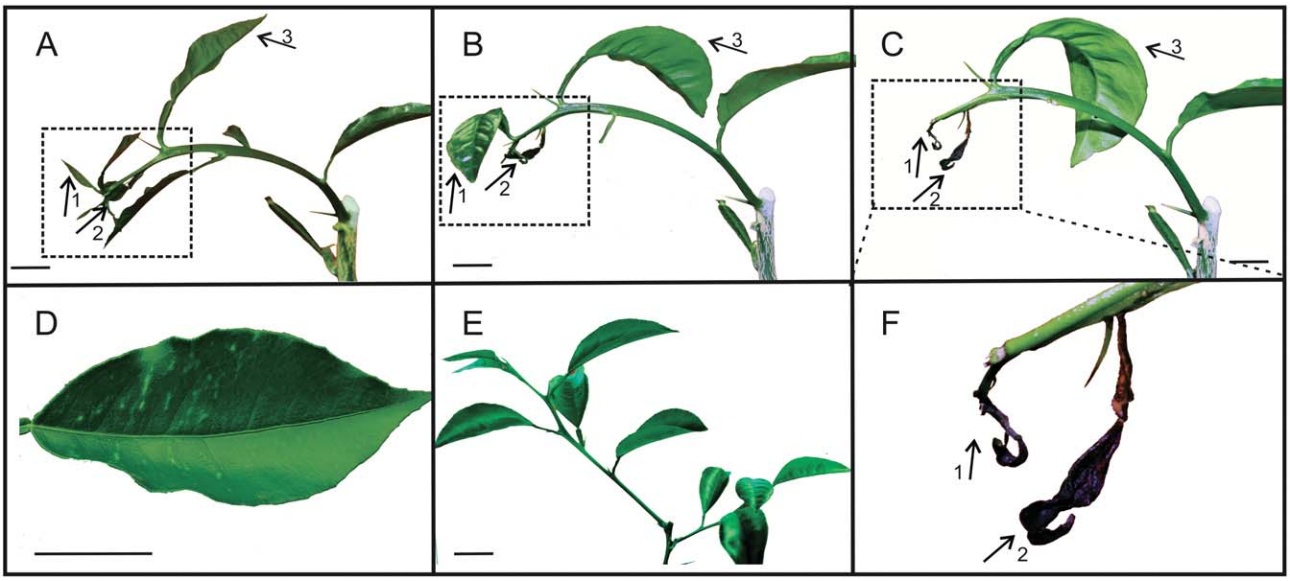

Fig. 1 Symptoms observed in *Citrus sinensis* plants infected with *Citrus psorosis virus* (CPsV) isolates used for microRNA (miRNA) and target analyses. (A–C, F) Young shoot displaying a progressive shock reaction caused by CPsV-90-1-1, including epinasty and, finally, necrosis of the leaves. Leaves 1 and 2 show progressive necrosis (time between A and C, 15 days). (D) Flecking symptoms caused by CPsV 90-1-1 isolate in leaves of plants of the same developmental stage. (Leaves from the CPV4-infected plants show similar flecking symptoms.) (E) healthy shoots. (F) Shock reaction in detail (inset). Scale bars: 5 mm equals 10 mm.

case of the shock reaction, samples were collected when young flushes began to bend and just before the onset of necrosis (Fig. 1A).

Most analysed miRNAs (seven of ten; miR156, miR167, miR169, miR171, miR172, miR393 and miR403) showed a decreased accumulation in infected relative to non-infected tissues (Fig. 2A, B). The mature miRNA level ranged from a 1.2- to 2.8-fold reduction compared with the healthy sample. miR156 and miR171 were the most drastically altered miRNAs. In particular, miR156 showed a reduction in the accumulation of the mature miRNA species present in flecking samples, from 1.5- to two-fold compared with the healthy control (in both isolates), whereas tissue displaying shock showed a more severe decrease of 2.8-fold (Fig. 2B). Differences between shock and flecking samples were significant for miR156. miR171 showed similar decreasing levels and association pattern, but differences between shock and flecking samples were not significant. miR167 also displayed a drastic down-regulation on virus infection with similar levels for all infected samples (around two-fold). miR169 showed a detectably reduced level in flecking samples, but no significant differences for the shock sample. Finally, miR172, miR393 and miR403 showed lower levels of down-regulation in some of the infected samples. In particular, miR172 showed a faint band in Northern blots, but the results from three independent experiments exhibited similar accumulation patterns (Fig. 2B).

In summary, we found that the infection of citrus plants with two CPsV isolates caused a reduction in the accumulation level of several miRNAs, and that miR156, miR171 and miR167 were the most highly down-regulated miRNAs.

Induction of miRNA target expression in CPsV-infected *C. sinensis* plants

To assess whether mRNA target levels of the most strongly down-regulated miRNAs were also affected after CPsV infection, we selected the following genes to provide further analysis: *Squamosa promoter-binding protein-like* (*SPL*) *9* and *13*, *Scarecrow-like 6* (*SCL6*) and *Auxin response factor* (*ARF*) *6* and *8*. *SPL9* and *SPL13* (miR156 targets) are involved in the juvenile to adult phase transition, abiotic stress responses, symptom expression and defence (Cardon *et al*., 1997, 1999; Cui *et al*., 2014; Klein *et al*., 1996; Padmanabhan *et al*., 2013), whereas *SCL6* (miR171 target) is involved in gibberellic acid responses that control flowering and regulate apical meristem development (Bolle, 2004) and chlorophyll biosynthesis (Ma *et al*., 2014). Finally, *ARF6* and *ARF8* (miR167 targets) regulate flower development caused by VSR expression in *A. thaliana* plants (Jay *et al*., 2011; Wu *et al*., 2006). These transcripts are targets in *A. thaliana* as well as in citrus (Song *et al*., 2010a).

RNA extracts obtained from the same foliar samples as used for miRNA quantification were subjected to quantitative reverse transcription-polymerase chain reaction (qRT-PCR) (Fig. 3). *SPL9* showed an up-regulation of approximately two-fold, compared with the healthy control, in CPsV 90-1-1-infected leaves expressing flecking symptoms. Samples from plants infected with the

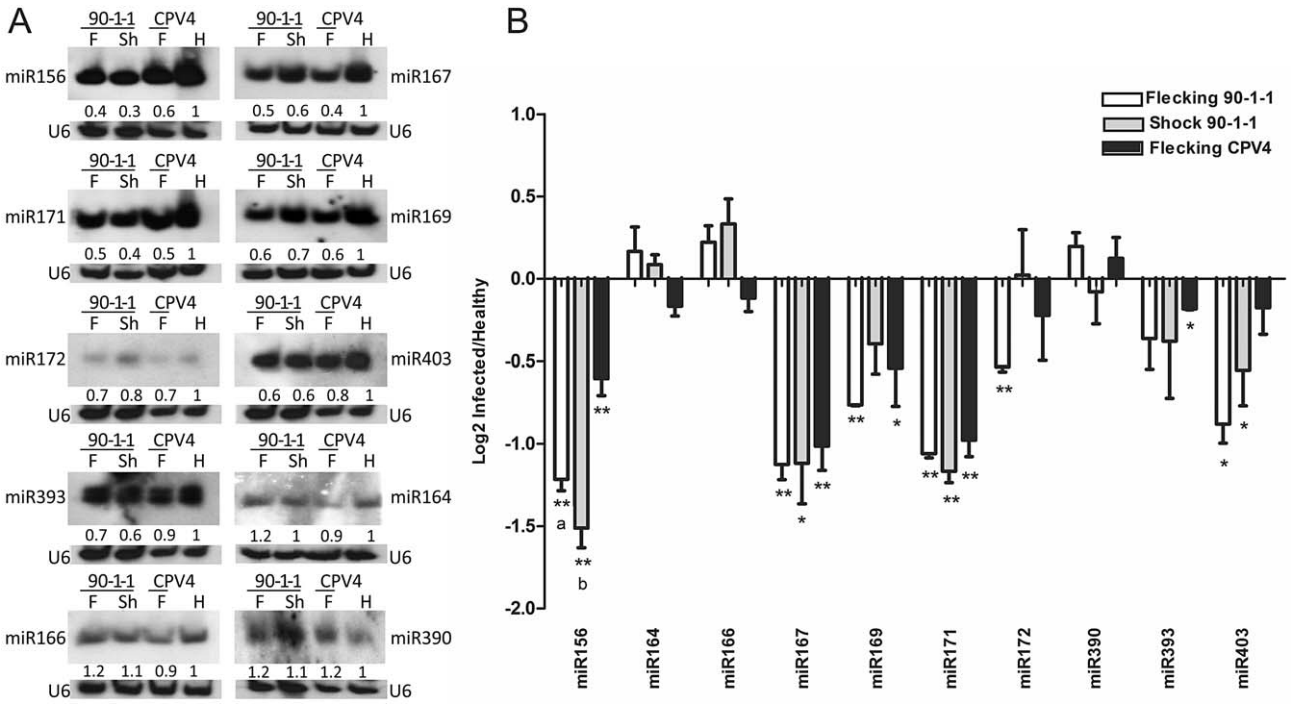

Fig. 2 Accumulation of endogenous microRNAs (miRNAs) in *Citrus sinensis* plants infected with *Citrus psorosis virus* (CPsV) 90-1-1 or CPV4 isolate. (A) Representative Northern blot analysis of various conserved miRNAs after infection. F, flecking symptom; H, healthy leaves; Sh, shock reaction symptom. Lower panels show U6 normalization. Ratios between band densities of each miRNA and U6 were calculated. (B) Relative accumulation of miRNA compared with healthy leaves (H = 1) (mean values and standard error of miRNA level of three independent experiments). The graphs were plotted as $\log_2$ of the infected/healthy sample ratios. Differences between two groups were tested with a two-tailed paired *t*-test. * and ** indicate $P < 0.05$ and $P < 0.01$ values, respectively, in comparison with the healthy group. a and b indicate $P < 0.05$ between F and Sh, respectively.

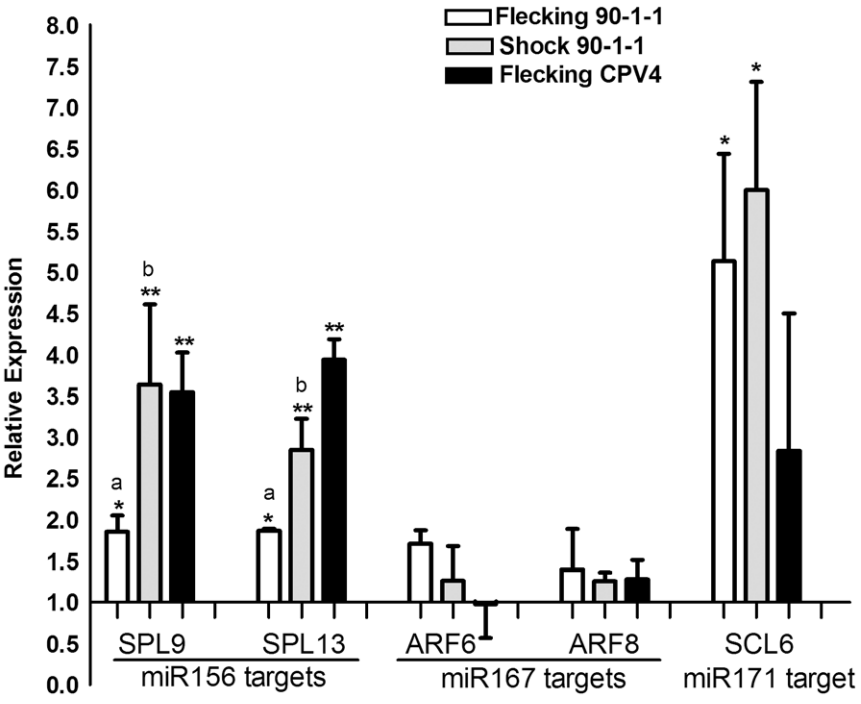

Fig. 3 Accumulation of microRNA (miRNA) target transcripts in *Citrus sinensis* plants infected with *Citrus psorosis virus* (CPsV) 90-1-1 or CPV4 isolate. Quantitative reverse transcription-polymerase chain reaction (qRT-PCR) assays were performed to determine the expression levels of *Squamosa promoter-binding protein-like 9* (*SPL9*) and *SPL13* (miR156 targets), *Auxin response factor 6* (*ARF6*) and *ARF8* (miR167 targets) and *Scarecrow-like 6* (*SCL6*) (miR171 target). Mean values and standard errors of three independent experiments are shown. Healthy samples are established as 1. Differences from the healthy samples were tested using a two-tailed paired *t*-test. * and ** indicate $P < 0.05$ and $P < 0.01$ values, respectively. a and b indicate $P < 0.05$ value between F and Sh, respectively.

same isolate, but expressing shock reaction, accumulated about 3.5-fold higher levels of miRNAs. Similar increases resulted in the accumulation of *SPL9* transcripts from CPV4-infected leaves expressing flecking symptoms. The behaviour of *SPL13* was comparable, but CPV4 samples showed a more striking up-regulation of about four-fold. *ARF6* and *ARF8* did not show significant changes in any sample; these genes may be regulated at a translational level or in specific tissues. *SCL6* levels were more than five times higher in the CPsV 90-1-1-infected samples (flecking and shock). The average levels of the *SCL6* transcript were also higher, but not significantly, in CPV4-infected samples.

The expected negative correlation between miRNA accumulation and target transcripts was observed in three of the five evaluated targets (*SPL9*, *SPL13* and *SCL6*) when infected plants and healthy controls were compared. We could not establish a correlation between the two virus isolates or between the two types of symptom when *SPL* transcript abundance was evaluated. For *SCL6*, which was the most altered transcript, we detected an apparent association pattern between CPsV 90-1-1-infected samples. These plants exhibited a significantly higher level of *SCL6* compared with the CPV4-infected samples. *ARF* transcripts appeared not to be post-transcriptionally regulated by miR167. Another possible explanation could be that its effect is either masked by the mixtures of different cell types with antagonistic regulation or rapidly regulated by feedback mechanisms.

In summary, CPsV infection down-regulates the accumulation of several mature miRNAs, with a consequent increase in some mRNA target levels, in particular *SPL9*, *SPL13* and *SCL6*.

Alteration of pre-miR156 and pre-miR171 processing in CPsV-infected *C. sinensis* plants

The reduced levels of mature miRNAs after CPsV infection could be explained primarily by three mechanisms: (i) a reduction in the pri-miRNA transcription level; (ii) an alteration of processing of pri-miRNA into mature miRNA; and (iii) an active degradation of the mature miRNA.

To test the first hypothesis, we designed primers for the miR156*a* primary transcript sequence (pri-miR156*a*) from *C. sinensis*. This transcript of 1306 nucleotides, present in the Citrus Genome database, includes the pre-miR156*a* sequence (Fig. 4A). The accumulation of pri-miR156*a* was quantified by qRT-PCR, and remained apparently unaltered in infected leaves compared with healthy samples (Fig. 4B). To explore the possibility of pre-miRNA processing alteration (second proposed mechanism), we analysed the intermediate species generated during pre-miR156 processing by Northern blot. We have analysed previously the secondary structures of all members of the pre-miR156 family, and the data correlate with a loop-to-base processing model (Fig. S1, see Supporting Information), which is coincident with the *A. thaliana* pre-miR156 processing mechanism confirmed *in vitro* (Bologna *et al*., 2013b; Liu *et al*., 2012). Among the entire analysed set of pre-miRNAs (data not shown), unprocessed pre-miR156 and processing intermediates (F1 + m) were clearly detected using a probe against the mature sequence (m) (Fig. 5A, B). In *A. thaliana*, two species excised by the first cut of DCL1 have been described: a 42-nucleotide fragment including the small structured loop or upper loop, and the two arms of 45 nucleotides comprising the lower stem and mature or star sequences. A second cut renders the mature sequence (21 nucleotides) and the lower stem separately. Analogous cuts in *C. sinensis* pre-miR156*a* (143 nucleotides) (Fig. 5B) would also render two putative intermediates in the first cut of the proposed loop-to-base mechanism: the 41-nucleotide upper loop (F3) and two 51-nucleotide sequences comprising the lower stem and mature or star sequences (F1 + m, F2 + m*). The second cut excised the mature and lower stem species separately. Infected leaves displayed a reduced accumulation of intermediate

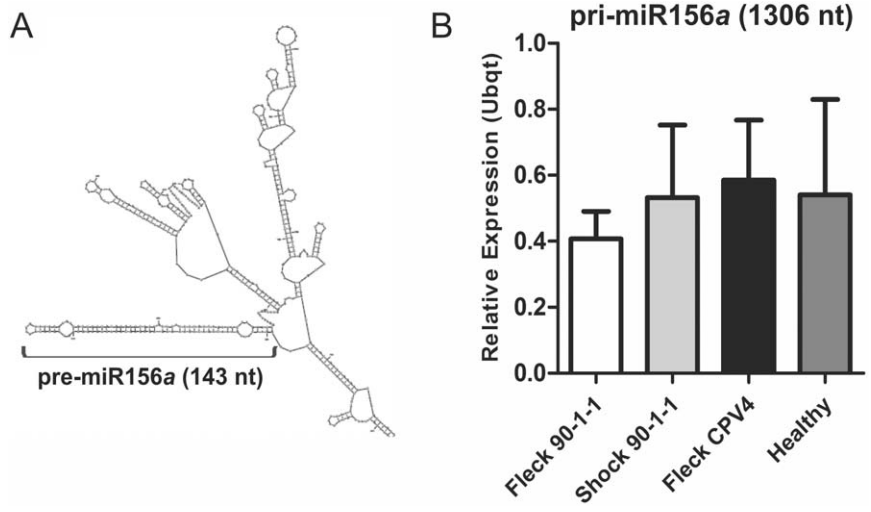

Fig. 4 *Citrus sinensis* miR156*a* primary transcript (pri-miR156*a*). (A) Predicted secondary structure of pri-miR156*a* (part of the molecule is shown). pre-miR156*a* stem loop is indicated. (B) Quantitative reverse transcription-polymerase chain reaction (qRT-PCR) assays were performed to determine the accumulation levels of pri-miR156*a* in infected (Fleck 90-1-1; Shock 90-1-1; Fleck CPV4) and healthy samples. nt, nucleotide; Ubqt, ubiquitin.

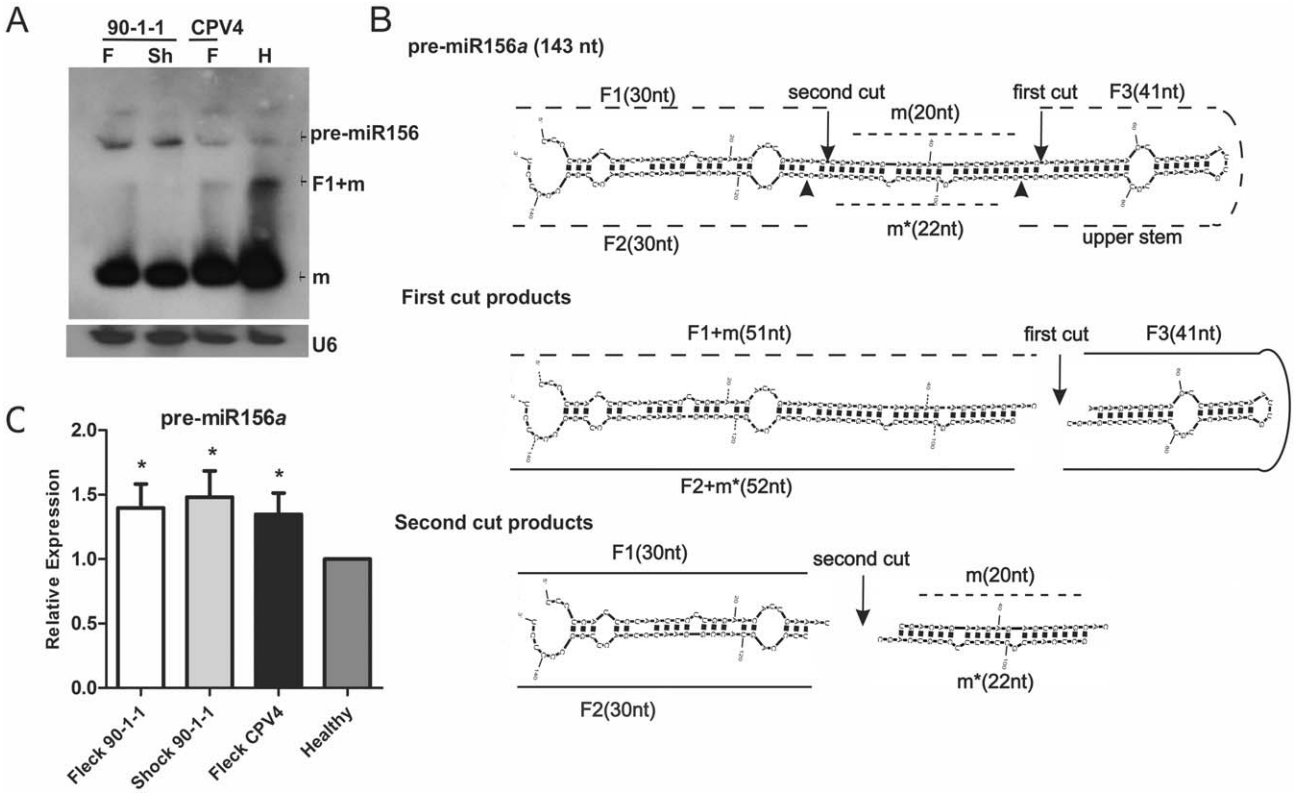

Fig. 5 pre-miR156 processing in *Citrus psorosis virus* (CPsV)-infected *Citrus sinensis*. (A) Northern blot analysis of pre-miR156 and processing intermediates after infection with CPsV 90-1-1 or CPV4 isolate using a probe against the mature species. F, flecking symptom; H, healthy leaves; Sh, shock reaction symptom. Unprocessed precursor (pre-miR156), intermediate processing fragments (F1 + m) and mature species (m) are indicated with arrows on the right. Lower panel shows U6 normalization. (B) Predicted secondary structure of *C. sinesis* pre-miR156*a* and predicted fragments from DICER-like 1 (DCL1)-catalysed processing. Fragments are named F1 and F2 (arm fragments), F3 (loop fragment) and m/m* [miRNA and miRNA* fragments of 20 and 22 nucleotides (nt)]. First and second cut products of processing are detailed. Labelled and unlabelled molecules in the Northern blot are indicated with broken and full lines, respectevely. (C) Quantitative reverse transcription-polymerase chain reaction (qRT-PCR) assays were performed to determine the accumulation levels of pre-miR156*a* in the same samples as (A). * indicates significant differences from healthy control samples at $P < 0.05$ using a two-tailed paired *t*-test.

(F1 + m) processing fragments compared with healthy leaves, and an increase in the unprocessed precursor (Fig. 5A). qRT-PCR was performed using primers designed to quantify the unprocessed pre-miR156*a* (Fig. 5C). These assays showed a higher accumulation of the unprocessed species in infected samples. Reverse primers were designed specifically to detect the seven members of the *C. sinensis* pre-miR156 (*a*–*g*), but only three (*a*–*c*) were detected (Fig. S2, see Supporting Information). This result agrees with previous studies which describe these three as the most abundant members of the family (Xu *et al*., 2010).

Mature miR171 is also down-regulated by CPsV infection and has strong effects on *SCL6* target expression (Fig. 3). To evaluate whether the processing alteration is exclusive of miR156 or is also exerted by other precursors, we assessed pre-miR171*a* accumulation through qRT-PCR for the infected (CPsV 90-1-1 or CPV4) and healthy samples. Similar to the results described for pre-miR156*a*, these assays demonstrated a higher accumulation of the unprocessed precursors in the infected samples (Fig. 6).

The lower accumulation of mature and intermediate processing fragments (F1 + m) and the concomitant increase in unprocessed pre-miRNA level, without changes in the primary transcript levels, suggest that CPsV directly or indirectly interferes with miR156 processing. A similar accumulation of unprocessed species of pre-miR171*a* in infected samples suggests that the mechanism exerted by the virus is not restricted to one miRNA, but also extends to others.

Interaction of pre-miR156 and pre-miR171 with 24K viral protein

To examine whether CPsV proteins interact with pre-miR156 or pre-miR171, thus affecting the normal miRNA biogenesis processing, we performed RNA immunoprecipitation (RIP) assays. A previous analysis of the movement protein (54K) demonstrated that it has a bipartite nuclear localization signal (NLS) and localizes in the plasmodesmata and nucleus (confocal microscope observations;

confocal laser scanning microscopy, CLSM) (Robles Luna *et al*., 2013). A nuclear export signal (NES) was also predicted for the 24K protein. To define the localization of this protein, we performed transient expression of 24K enhanced green fluorescent protein (eGFP)-fused protein (24K:eGFP) in *N. benthamiana* epidermal cells. Through CLSM, we found that 24K:eGFP co-localized with co-expressed free monomeric red fluorescent protein (mRFP) in the nucleus (Fig. 7). Because of this evidence, we selected these two CPsV proteins to assay the association with miRNA precursors that are also present in the nucleus.

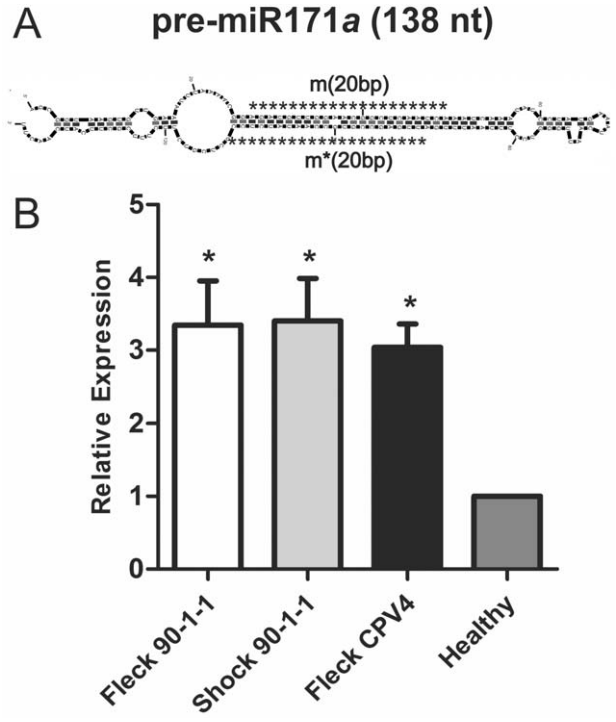

Fig. 6 *Citrus sinensis* pre-miR171*a*. (A) Predicted secondary structure of pre-miR171*a*. miRNA and miRNA* sequences of 20 nucleotides (nt) are indicated with asterisks. (B) Quantitative reverse transcription-polymerase chain reaction (qRT-PCR) assays were performed to determine the accumulation levels of pre-miR171*a* in infected (Fleck 90-1-1; Shock 90-1-1; Fleck CPV4) and healthy samples. * indicates significant differences from healthy control samples at $P < 0.05$ using a two-tailed paired *t*-test.

GFP-fused forms of CPsV 54K (54K:eGFP) (Robles Luna *et al*., 2013) and 24K (24K:eGFP; generated here) proteins were expressed in *N. benthamiana* leaves, and total RNA was recovered by immunoprecipitation with anti-GFP from tissue expressing these CPsV proteins. *Nicotiana benthamiana* pre-miR156*a* and pre-miR171*a* were detected in the GFP immunoprecipitates and quantified by qRT-PCR. Non-fused GFP and mRFP were also tested as controls. The 24K and 54K proteins were also co-expressed to test the putative additive effect. The 24K:eGFP protein expressed alone or co-expressed with 54K:eGFP showed higher levels of enrichment of pre-miR156*a* (4.5- and 3.5-fold, respectively) compared with the non-fused GFP control (Fig. 8A); 54K:eGFP expressed alone showed a non-significant fold enrichment of 0.5. For pre-miR171*a*, 24K:eGFP expressed alone or co-expressed with 54K:eGFP showed a significant enrichment of 1.9- and 1.4-fold, respectively (Fig. 8B); 54K:eGFP expressed alone showed a non-significant 0.4-fold enrichment. The endogenous ubiquitin transcript was also tested, and no significant difference in enrichment was detected between fused viral proteins and the mRFP control (Fig. 8A, B). The presence and integrity of the viral proteins were confirmed by Western blots of input and immunoprecipitated fractions (Fig. S3, see Supporting Information).

These results suggest a direct or indirect interaction between pre-miR156*a* and pre-miR171*a* with 24K in *N. benthamiana*. This interaction could affect miRNA processing and consequently generate the observed higher accumulation of precursors and the reduction in mature miRNAs in citrus.

DISCUSSION

Plant virus infections often produce a variety of disease symptoms that can have a dramatic impact on agricultural production. Different molecules, including miRNAs, have emerged as candidates that modulate complex host–pathogen interactions (Bazzini *et al*., 2009; Carrington and Ambros, 2003; Dorokhov Iu, 2007; Palatnik *et al*., 2003). Because miRNAs can control the expression of proteins, they may influence the cellular tropism of viruses, modulate viral infectivity and play a crucial role in the induction of appropriate antiviral immune responses. It is therefore not surprising that RNA viruses may regulate the expression

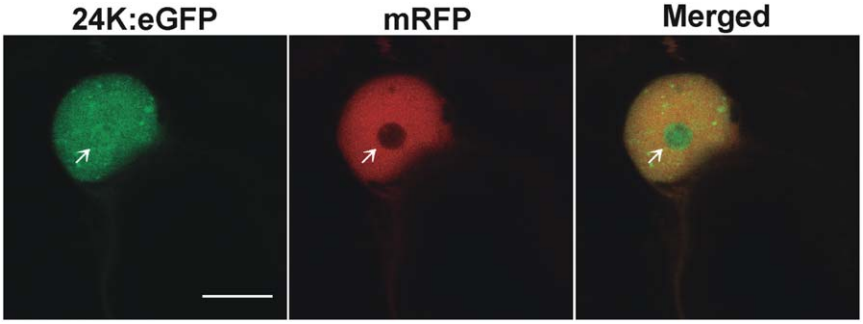

Fig. 7 Nuclear localization of 24K:eGFP protein in *Nicotiana benthamiana*. (A) Co-expression of *24K:eGFP* with free mRFP (nuclear cytoplasmic marker) at 3 days post-agroinfiltration in *N. benthamiana* epidermal cells. Merged image is shown. Scale bar, 10 μm. Arrows indicate the nucleolus. eGFP, enhanced green fluorescent protein; mRFP, monomeric red fluorescent protein.

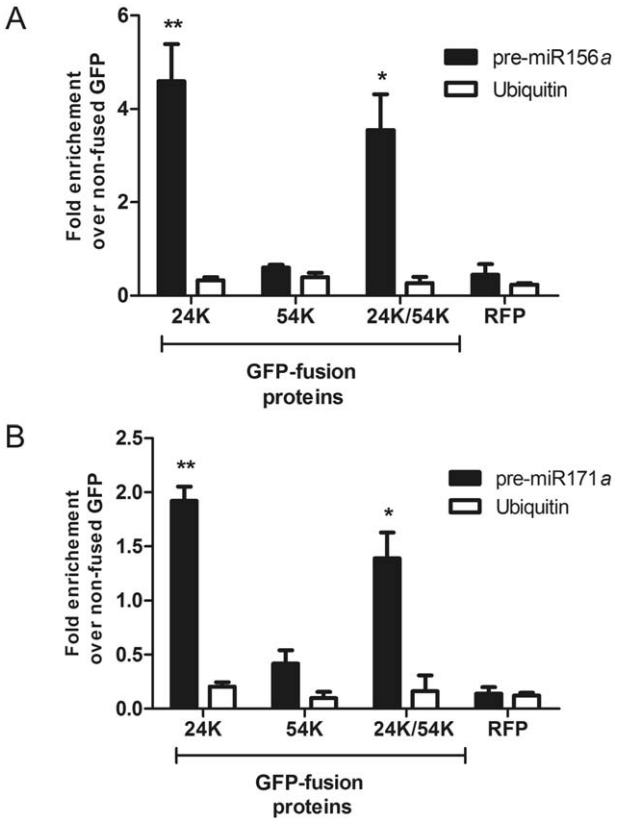

Fig. 8 Co-immunoprecipitation analysis of precursors associated with 24K and/or 54K proteins from *Citrus psorosis virus* (CPsV) in *Nicotiana benthamiana*. Transiently expressed GFP-fusion proteins were immunoprecipitated with an anti-GFP antibody. RNA samples eluted from the protein–RNA complexes were analysed by quantitative reverse transcription-polymerase chain reaction (qRT-PCR) to determine the accumulation levels of *N. benthamiana* pre-miR156*a* (A) or pre-miR171*a* (B). Fold enrichment of the immunoprecipitated (IP) precursors was calculated by comparing the amount of RNA in the input vs. RNA in the IP (ΔCT) corrected by the input dilution factor. This value was compared for each specific IP (24K, 54K or the co-expressed 24K/54K) over the mock IP (non-fused GFP). The resulting value was used to calculate the fold enrichment [2(ΔΔCT)]. Mean values and standard errors are shown ($n = 3$). Statistical analysis was performed using a two-tailed paired *t*-test; * and ** indicate significant differences from RFP control sample at $P < 0.05$ and $P < 0.01$ values, respectively. GFP, green fluorescent protein; RFP, red fluorescent protein.

of specific miRNAs for efficient replication as an ever-evolving survival strategy (Swaminathan *et al*., 2013). Infections can lead to the up- or down-regulation of host miRNAs, and can consequently produce massive gene expression changes in the host. It remains uncertain whether all the changes in miRNA pathways are adaptive strategies of viruses to exploit host gene regulation and, finally, to elude resistance responses, or whether they are just side-effects caused by shared components of silencing and miRNA pathways. Various reports support the adaptive hypothesis. For instance, *Turnip mosaic virus* infection induces Brassica miR1885, whose target is the *Toll/interleukin-1 receptor-nucleotide-binding site-leucine-rich repeat* (*TIR-NBS-LRR*) class of disease resistance transcripts (He *et al*., 2008). This is in line with the hypothesis that miRNAs function as master regulators of *NBS-LRR*s via the targeting of highly conserved motifs (Zhai *et al*., 2011). Other common targets, such as SPL transcription factors, that ultimately modulate similar viral resistance genes (*TIR-NB-LRR N immune receptor*), are also candidates for such types of viral adaptive evasion of plant defence (Padmanabhan *et al*., 2013).

In this work, we have demonstrated that the levels of a group of conserved miRNAs previously implicated in symptom development (Bazzini *et al*., 2007) are reduced in *C. sinensis* plants infected with two different isolates of CPsV. Triboulet *et al*. (2007) first described the down-regulation of two cellular miRNAs during human immunodeficiency virus (HIV) infection in human cells. They proposed that the reduction in these miRNAs constitutes a viral mechanism for boosting the levels of proteins required for replication and spread. In this study, we report an almost three-fold reduction in miR156, miR171 and miR167 after CPsV infection. Some of their target transcripts (*SPL*s, *SCL*s and *ARF*s) have been reported previously to be related to symptom expression and defence (Gao *et al*., 2013; Jay *et al*., 2011; Padmanabhan *et al*., 2013). In the present study, we found that *SPL*s and *SCL* were concomitantly up-regulated in CPsV-infected plants, but could not find a general correlation between the expression patterns of all the assessed miRNA target transcripts with the two types of exhibited symptom or with one of the two distant CPsV isolates.

Most reports including VSR-mediated mechanisms responsible for miRNA alterations involve effector pathways that comprise already processed (mature) miRNA species; the biogenesis and processing of precursors, however, may also be affected by viral infection. For example, Bazzini *et al*. (2009) reported transcriptional alterations of *A. thaliana* miR164 by ORMV infection. Lu & Cullen (2004) demonstrated that the adenovirus VA1 RNA inhibits the biogenesis of miRNAs by hampering the nuclear export of pre-miRNA precursors and by preventing Dicer function through binding. Here, we have demonstrated that citrus plants infected with CPsV show a reduction in pre-miR156 and pre-miR171 processing, which leads to greater amounts of precursors and decreased amounts of mature species. Furthermore, the alteration of pri-miRNA156*a* levels by transcriptional activation of the *MIR156a* gene can be discarded, which supports the hypothesis that pre-mi156*a* processing is the affected pathway.

Two main hypotheses emerge to explain the processing alterations: (i) the viral proteins can inhibit directly components of the miRNA processing machinery; and (ii) the viral protein can bind miRNA precursors impeding its processing. In relation to the first hypothesis, the dsRNA-binding protein HYL1, which interacts with DCL1 and assists the efficient and precise cleavage of miRNA precursors (Kurihara *et al*., 2006), is crucial for the

efficient processing of miR156*a* (Liu *et al*., 2012). Other studies by Li *et al*. (2012) have revealed that most of the miRNAs are down-regulated in *A. thaliana hyl1* mutants and that miR156*a-f* is the most down-regulated, reaching more than 10-fold reduction compared with wild-type plants. Here, we showed that miR156 accumulation is the most affected by CPsV infection and that miR156 processing is also clearly altered. Therefore, a CPsV protein or a complex of CPsV proteins could interact with HYL1 during infection, thus limiting its function and ultimately affecting the processing of miR156. The nuclear localization of 24K (this study) and 54K (Robles Luna *et al*., 2013) also favours the idea of an interaction with DCL1, HYL1, SERRATE and/or components of the cap-binding complex, which are present in the same compartment. In relation to the second hypothesis, the immunoprecipitation experiments revealed an association between 24K and pre-miR156*a* or pre-miR171*a*, thus suggesting an interaction of these proteins with miRNA precursors in the nucleus. Other results have also shown that 24K and 54K can potentially bind synthetic long dsRNAs *in vitro* (C. A. Reyes, IBBM, La Plata, Argentina. unpublished data), which supports direct interaction impeding the normal processing of the miRNA precursor by the biogenesis machinery. However, the role of CPsV viral proteins in the alteration of miRNA processing by both mechanisms cannot be discarded.

Recent reports involving miR156 in responses to different stresses may explain the observed effect in miR156 and its targets. Cui *et al*. (2014) associated miR156 and *SPL9* accumulation with abiotic stress tolerance in *A. thaliana*. Moreover, SPL transcription factors play a regulatory role in the resistance to the bacterial pathogen *Pseudomonas syringae* in *A. thaliana* and to TMV infection in *N. benthamiana*. These factors appeared to be implicated in the transcription of key immune response genes involved in the induction of the hypersensitive response and programmed cell death (HR-PCD) (Padmanabhan *et al*., 2013).

We have reported here that infected young shoots, previous to necrosis, accumulate large amounts of *SPL* transcripts, which is concomitant with a decrease in mature miR156 caused by viral-mediated misprocessing. The involvement of these transcription factors in the activation of genes related to necrosis and PCD in CPsV-infected citrus plants would be an interesting feature to assess. Similarly, the accumulation of *SCL* transcripts (the most affected target in CPsV 90-1-1-infected plants) and the reduction in mature miR171 can be associated with chlorophyll biosynthesis regulation, as described by Ma *et al*. (2014). In that report, it is proposed that light promotes miR171 expression, which leads to a concomitant decrease in *SCL* expression with an increase in chlorophyll biosynthesis (Ma *et al*., 2014). In the case of CPsV 90-1-1-infected plants, larger amounts of miR171-targeted SCL6 could negatively regulate chlorophyll biosynthesis, thus contributing to the chlorosis manifested in CPsV-infected leaves.

As mentioned previously, there are a few examples of DNA viruses (adenoviruses) interfering with pre-miRNA processing (Lu and Cullen, 2004), but no study has been described in plant viruses, most with exclusive cytoplasmic cycles. In this study, we assessed this mechanism for CPsV, a segmented RNA virus that has a nuclear component affecting miRNA processing. Further studies are needed to fully characterize the molecular basis of the proposed interaction between CPsV viral proteins and miRNA precursors and/or the components of the biogenesis machinery in *C. sinensis*. Our results also provide insight into the host–pathogen interaction of a worldwide important crop, sweet orange. Little is known about citrus miRNA regulation, role and function, or about the molecular mechanisms of viral infection. The elucidation of the role of miRNAs during symptom expression and pathogenesis in citrus would also help in the design of new molecular approaches to reduce economic losses.

EXPERIMENTAL PROCEDURES

Plant citrus material and CPsV isolates

The CPsV isolates used in this study were the Argentine CPsV 90-1-1 (INTA, Concordia, Argentina) (García *et al*., 1993) and CPV4 (USA) (Garnsey *et al*., 1976). CPV4 is the most distant isolate among the three groups established by Martin *et al*. (2006). Pineapple sweet orange plants [*Citrus sinensis* (L.) Osbeck] were infected by graft inoculation using a small chip taken from infected bark tissue. The chip was inserted in the stem (Roistacher, 1991).

Virus detection

For CPsV infection analysis, triple antibody sandwich-enzyme-linked immunosorbent assay (TAS-ELISA) or dot blots were performed. TAS-ELISA-horseradish peroxidase (TAS-ELISA-HRP) was performed as described previously by Zanek *et al*. (2006) using total protein extracted from 200 mg of leaf tissue. Dot blots were performed using serial dilutions (1 μg to 1 ng) of all samples. Probes for the *cp* gene were used and hybridizations were performed according to Reyes *et al*. (2009).

Plasmid constructs and bacterial strains

To express gfp-24K fusion protein (pB7FWG2-24K), we cloned the open reading frame (ORF) without the stop codon into pCR8/GW/TOPO (Invitrogen, Carlsbad, CA, USA.). The resulting entry plasmids were digested with *Xho*I and recombined with destination vectors pB7FWG2 (Karimi *et al*., 2002) using LR clonase mix (Invitrogen) according to the manufacturer's instructions. The correct cloning and insert orientation were confirmed by sequencing. The verified construct was transferred to *Agrobacterium tumefaciens* strain GV3101 by electroporation.

miRNA isolation and detection

For miRNA analysis by Northern blot, total RNA was extracted from citrus leaves using TriReagent® (Molecular Research Center, Inc. Cincinnati, OH,

USA.). Total RNA from each sample was separated in denaturing polyacrylamide gels, transferred to a positively charged nylon membrane (Roche Diagnostics Corporation, Indianapolis, IN, USA) by a Bio-Rad (Hercules CA, USA) transfer unit and chemically fixated according to Pall and Hamilton (2008). Probes were ^{32}P-radiolabelled oligodeoxynucleotides complementary to the mature miRNA or to the U6 snRNA sequence, which was included as a loading control (Table S1). Hybridizations were performed at 50 °C overnight and signals were detected by autoradiography. Band intensity was quantified using ImageJ software. Data from U6 quantification were used for normalization. The value for the miRNA species in healthy plants was set at 1.0 (Fig. 2A). The data shown in Fig. 2B are the mean of three independent experiments.

Target detection

For qRT-PCR analysis of the target transcripts, we synthesized first-strand cDNA from total DNAse-treated RNA using oligodT and MMLV (Promega Madinson, WI, USA.). cDNA was used as a template for PCRs. PCR was performed with an iCycler iQ (Bio-Rad) and SYBR-GREEN Master mix (Bio-Rad) in a reaction held at 95 °C for 5 min, then 44 cycles of 20 s at 95 °C, 30 s at 56 °C and 20 s at 72 °C, followed by 10 min at 72 °C. Gene-specific primers are indicated in Table S1. The presence of a unique product of the expected size was verified on ethidium bromide-stained agarose gels. The absence of contaminant genomic DNA was confirmed in reactions with DNAse-treated RNA as the template. *Citrus sinensis* ubiquitin amplification was used to normalize the amount of template cDNA. The reproducibility of the assay was monitored by running technical triplicates. At least three biological replicates were performed. Primers for *C. sinensis* target detection were designed using citrus sequences deposited in GenBank and the citrus expressed sequence tag (EST) database (Version 1.20 HarvEST:Citrus) (Table S1). The *SPL* sequences come from *Poncirus trilfoliata* ESTs and were validated as a miR156 target by RNA ligase-mediated 5'-rapid amplification of cDNA ends (5'-RACE) (Song *et al*., 2010a). *SPL9* (FJ502237.1) is a homologue of AT2G42200 and SPL13 (FJ502238.1) is a homologue of AT5G50570. The *SCL6* (GQ505957.1) sequence belongs to *Citrus trifoliata* and is a homologue of the GRAS family of the transcription factor AT4G00150.1. The *ARF6* (UNIGEN-15948, HarvEST:citrus) and *ARF8* (UNIGEN-30530, HarvEST:citrus) sequences from *C. sinensis* are homologues of AT1G30330 and AT5G37020. The ubiquitin transcript GU362416.1 from *C. sinensis* was used as an internal control (Boava *et al*., 2011).

pri-miRNA and pre-miRNA detection and bioinformatic analysis

The qRT-PCR analyses of pri-miR156 and pre-miR156 or pre-miR171 were performed as described previously for target transcripts using specific primers (Table S1). The annealing temperature was 49 °C. The sequence from pri-miR156*a* (orange1.1g034943m|PACid:18109087) was obtained from the transcript dataset of the Citrus Genome database. The sequences from pre-miR156 and pre-miR171 families were taken from Xu *et al*. (2013). Secondary structures were obtained using the Mfold program (Zuker, 2003), with default parameters. In Fig. S1, the proximal end of the miRNA/miRNA* duplex was defined as position +1. Matched positions were rated as 0, whereas unpaired positions were considered as +1. The average for all the family members was calculated.

Immunoprecipitation of RNA-binding proteins (RIP)

pB7FWG2-24K (generated in this study; see 'Plasmid constructs and bacterial strains' section) and/or pB7FWG2-54K (Robles Luna *et al*., 2013) constructs expressing eGFP-fused proteins were transiently expressed in *N. benthamiana* plants using *A. tumefaciens* GV3101 strain. Cells were harvested by centrifugation, suspended in water to a final optical density at 600 nm (OD_{600nm}) of 0.4 and injected into the abaxial side of the leaf using a syringe without a needle. Leaves were observed in a Nikon fluorescence microscope (Eclipse Ti) (Nikon Corporation, Tokyo, Japan) under UV light at 4 days post-agroinfiltration (dpai). Non-fused eGFP and mRFP constructs were used as controls (Pena *et al*., 2012; Robles Luna *et al*., 2013).

The agroinfiltrated leaves were cross-linked *in vivo* with 1% formaldehyde in phosphate-buffered saline (PBS) (pH 7.4) by vacuum infiltration for 20 min at room temperature to fix protein–nucleic acid. The reaction was stopped with 125 mM glycine. Co-immunoprecipitation assays were performed with GFP-Trap®_A according to the manufacturer's instructions (Chromotek, Planegg-Martinsried Germany) with minor modifications. Total plant proteins were extracted with modified lysis buffer supplemented with 0.1% sodium dodecylsulfate (SDS), 1% Triton, 1% sodium deoxycholate, 5 mM dithiothreitol (DTT) and 50 U of RNAsin (Promega). The protein extracts were diluted with dilution buffer without Tween 20 to reduce the detergent concentration to 0.15%. An aliquot of the dilution was saved as input. The extracts were incubated with 20 μL of GFP-Trap A slurry for 1 h at 4 °C. After centrifugation at 3000 ***g*** and 4 °C for 5 min, the agarose beads were washed four times with ice-cold washing buffer supplemented with 0.1% SDS, 0.5% sodium deoxycholate, 2 M urea and 2 mM DTT. Then, 400 μL of TriReagent® (Molecular Research Center, Inc.) was added to the agarose beads and to the saved input. Incubation of the agarose beads at 55 °C for 5 min allows reversion of formaldehyde cross-linking. RNA was extracted as described by the manufacturer for further cDNA synthesis. Immunoprecipitated proteins were recovered from TriReagent® organic phase.

The expression, size and integrity of the fusion proteins were confirmed by Western blot in the input and immunoprecipitated fractions as described previously by Robles Luna *et al*. (2013).

Fluorescence microscopy

CLSM was performed using a Zeiss (Oberkochen, Germany) LSM510 microscope with a C-Apo-chromat (63/1.2 W Korr) water objective lens in multitrack mode, excitation/emission wavelengths of 488 nm/505–550 nm for eGFP and 561 nm/575–615 nm for mRFP, and LSM510 version 2.8 software. Images were processed with ImageJ software.

ACKNOWLEDGEMENTS

We thank Ing. Agr. Norma Costa and Pto. Agr. Fabián Ramos (Estación Experimental Agropecuaria, INTA-Concordia) and Tec. Agr. Claudio Mazo (IBBM, CCT-La Plata-CONICET-UNLP) for providing *C. sinensis* plants. We thank Eduardo Peña and Julia Sabio for critical reading of the manuscript.

MLG, CAR, EEO, FEM, GRL and MBB belong to the staff of IBBM, CCT-La Plata-CONICET-UNLP. AAB belongs to the staff of the Department

of Genetics, Yale University School of Medicine, and SA belongs to the staff of Instituto de Biotecnología, CICVyA-INTA. MLG, CAR and SA are recipients of research career awards from CONICET. EO, GRL and MBB are fellows of CONICET. This work was supported by grants from BID802-OC-AR PICT-1094, PICT-1726 and PICT-1019 ANPCyT, Argentina.

REFERENCES

Amin, I., Patil, B.L., Briddon, R.W., Mansoor, S. and Fauquet, C.M. (2011) A common set of developmental miRNAs are upregulated in *Nicotiana benthamiana* by diverse begomoviruses. *Virol. J.* **8**, 143.

Anderson, C. (2000) Presentation on the Argentinean certification program. *Proceedings of the Global Citrus Germplasm Network: 9th Congress of the International Society of Citriculture*, Orlando, Florida, USA 7-8 December 2000. Edited by Leo G., Albrigo, Published by Food and Agricultural Organization, United Nations, Seed and Genetic Resources Division. . Access at this publication is in: www.crec.ifas.ufl.edu/societies/ISC/gcgn/WG_3.PDF

Bartel, D.P. (2004) MicroRNAs: genomics, biogenesis, mechanism, and function. *Cell*, **116**, 281–297.

Bazzini, A.A., Hopp, H.E., Beachy, R.N. and Asurmendi, S. (2007) Infection and coaccumulation of tobacco mosaic virus proteins alter microRNA levels, correlating with symptom and plant development. *Proc. Natl. Acad. Sci. USA*, **104**, 12 157–12 162.

Bazzini, A.A., Almasia, N.I., Manacorda, C.A., Mongelli, V.C., Conti, G., Maroniche, G.A., Rodriguez, M.C., Distefano, A.J., Hopp, H.E., del Vas, M. and Asurmendi, S. (2009) Virus infection elevates transcriptional activity of miR164a promoter in plants. *BMC Plant Biol.* **9**, 152.

Boava, L.P., Cristofani-Yaly, M., Mafra, V.S., Kubo, K., Kishi, L.T., Takita, M.A., Ribeiro-Alves, M. and Machado, M.A. (2011) Global gene expression of *Poncirus trifoliata*, *Citrus sunki* and their hybrids under infection of *Phytophthora parasitica*. *BMC Genomics*, **12**, 39.

Bolle, C. (2004) The role of GRAS proteins in plant signal transduction and development. *Planta*, **218**, 683–692.

Bologna, N.G., Mateos, J.L., Bresso, E.G. and Palatnik, J.F. (2009) A loop-to-base processing mechanism underlies the biogenesis of plant microRNAs miR319 and miR159. *EMBO J.* **28**, 3646–3656.

Bologna, N.G., Schapire, A.L. and Palatnik, J.F. (2013a) Processing of plant microRNA precursors. *Brief Funct. Genomics*, **12**, 37–45.

Bologna, N.G., Schapire, A.L., Zhai, J., Chorostecki, U., Boisbouvier, J., Meyers, B.C. and Palatnik, J.F. (2013b) Multiple RNA recognition patterns during microRNA biogenesis in plants. *Genome Res.* **23**, 1675–1689.

Brodersen, P., Sakvarelidze-Achard, L., Bruun-Rasmussen, M., Dunoyer, P., Yamamoto, Y.Y., Sieburth, L. and Voinnet, O. (2008) Widespread translational inhibition by plant miRNAs and siRNAs. *Science*, **320**, 1185–1190.

Cardon, G., Hohmann, S., Klein, J., Nettesheim, K., Saedler, H. and Huijser, P. (1999) Molecular characterisation of the Arabidopsis SBP-box genes. *Gene*, **237**, 91–104.

Cardon, G.H., Hohmann, S., Nettesheim, K., Saedler, H. and Huijser, P. (1997) Functional analysis of the *Arabidopsis thaliana* SBP-box gene SPL3: a novel gene involved in the floral transition. *Plant J.* **12**, 367–377.

Carrington, J.C. and Ambros, V. (2003) Role of microRNAs in plant and animal development. *Science*, **301**, 336–338.

Cazalla, D., Yario, T. and Steitz, J.A. (2010) Down-regulation of a host microRNA by a Herpesvirus saimiri noncoding RNA. *Science*, **328**, 1563–1566.

Chapman, E.J., Prokhnevsky, A.I., Gopinath, K., Dolja, V.V. and Carrington, J.C. (2004) Viral RNA silencing suppressors inhibit the microRNA pathway at an intermediate step. *Genes Dev.* **18**, 1179–1186.

Chen, J., Li, W.X., Xie, D., Peng, J.R. and Ding, S.W. (2004) Viral virulence protein suppresses RNA silencing-mediated defense but upregulates the role of microRNA in host gene expression. *Plant Cell*, **16**, 1302–1313.

Cui, L.G., Shan, J.X., Shi, M., Gao, J.P. and Lin, H.X. (2014) The miR156-SPL9-DFR pathway coordinates the relationship between development and abiotic stress tolerance in plants. *Plant J.* **80**, 1108–1117.

Dorokhov Iu, L. (2007) [Gene silencing in plants]. *Mol. Biol. (Mosk)*, **41**, 579–592.

Dunoyer, P., Lecellier, C.H., Parizotto, E.A., Himber, C. and Voinnet, O. (2004) Probing the microRNA and small interfering RNA pathways with virus-encoded suppressors of RNA silencing. *Plant Cell*, **16**, 1235–1250.

Fang, Y. and Spector, D.L. (2007) Identification of nuclear dicing bodies containing proteins for microRNA biogenesis in living Arabidopsis plants. *Curr. Biol.* **17**, 818–823.

Fujioka, Y., Utsumi, M., Ohba, Y. and Watanabe, Y. (2007) Location of a possible miRNA processing site in SmD3/SmB nuclear bodies in Arabidopsis. *Plant Cell Physiol.* **48**, 1243–1253.

Gao, R., Wan, Z.Y. and Wong, S.M. (2013) Plant growth retardation and conserved miRNAs are correlated to Hibiscus chlorotic ringspot virus infection. *PLoS ONE*, **8**, e85476.

Garcia, M.L., Dal Bo, E., Grau, O. and Milne, R.G. (1994) The closely related citrus ringspot and citrus psorosis viruses have particles of novel filamentous morphology. *J. Gen. Virol.* **75** (Pt 12), 3585–3590.

García, M.L., Derrick, K.S. and Grau, O. (1993) Citrus psorosis associated virus and Citrus ringspot virus belong to a new virus group. In: *Proceedings of the 12th Conference of the International Organization of Citrus Virologists*. pp. 430–431. Edited by Moreno, P., da Graça, J.V. and Timmer, L.W., Published by IOCV, University of California, Riverside, CA.

Garnsey, S.M., Youtsey, C.O., Bridges, G.D. and Burnett, H.C.(1976) A necrotic ringspot-like virus found in a 'Star Ruby' grapefruit tree imported without authorization from Texas. *Proc. Fla. State Hortic. Soc.* **89**, 63–67.

Gregory, B.D., O'Malley, R.C., Lister, R., Urich, M.A., Tonti-Filippini, J., Chen, H., Millar A.H. and Ecker, J.R. (2008) A link between RNA metabolism and silencing affecting Arabidopsis development. *Dev. Cell*, **14**, 854–866.

Han, M.H., Goud, S., Song, L. and Fedoroff, N. (2004) The Arabidopsis double-stranded RNA-binding protein HYL1 plays a role in microRNA-mediated gene regulation. *Proc. Natl. Acad. Sci. USA*, **101**, 1093–1098.

He, X.F., Fang, Y.Y., Feng, L. and Guo, H.S. (2008) Characterization of conserved and novel microRNAs and their targets, including a TuMV-induced TIR-NBS-LRR class R gene-derived novel miRNA in Brassica. *FEBS Lett.* **582**, 2445–2452.

Jay, F., Wang, Y., Yu, A., Taconnat, L., Pelletier, S., Colot, V., Renou, J.P. and Voinnet, O. (2011) Misregulation of AUXIN RESPONSE FACTOR 8 underlies the developmental abnormalities caused by three distinct viral silencing suppressors in Arabidopsis. *Plos Pathog.* **7**, e1002035.

Jones-Rhoades, M.W., Bartel, D.P. and Bartel, B. (2006) MicroRNAS and their regulatory roles in plants. *Annu. Rev. Plant Biol.* **57**, 19–53.

Karimi, M., Inze, D. and Depicker, A. (2002) GATEWAY vectors for Agrobacterium-mediated plant transformation. *Trends Plant Sci.* **7**, 193–195.

Kasschau, K.D., Xie, Z., Allen, E., Llave, C., Chapman, E.J., Krizan, K.A. and Carrington, J.C. (2003) P1/HC-Pro, a viral suppressor of RNA silencing, interferes with Arabidopsis development and miRNA unction. *Dev. Cell*, **4**, 205–217.

Klein, J., Saedler, H. and Huijser, P. (1996) A new family of DNA binding proteins includes putative transcriptional regulators of the *Antirrhinum majus* floral meristem identity gene SQUAMOSA. *Mol. Gen. Genet.* **250**, 7–16.

Kurihara, Y. and Watanabe, Y. (2004) Arabidopsis micro-RNA biogenesis through Dicer-like 1 protein functions. *Proc. Natl. Acad. Sci. USA*, **101**, 12 753–12 758.

Kurihara, Y., Takashi, Y. and Watanabe, Y. (2006) The interaction between DCL1 and HYL1 is important for efficient and precise processing of pri-miRNA in plant microRNA biogenesis. *RNA*, **12**, 206–212.

Lakatos, L., Csorba, T., Pantaleo, V., Chapman, E.J., Carrington, J.C., Liu, Y.P., Dolja, V.V., Calvino, L.F., Lopez-Moya, J.J. and Burgyan, J. (2006) Small RNA binding is a common strategy to suppress RNA silencing by several viral suppressors. *EMBO J.* **25**, 2768–2780.

Lee, Y., Kim, M., Han, J., Yeom, K.H., Lee, S., Baek, S.H. and Kim, V.N. (2004) MicroRNA genes are transcribed by RNA polymerase II. *EMBO J.* **23**, 4051–4060.

Li, S., Yang, X., Wu, F. and He, Y. (2012) HYL1 controls the miR156-mediated juvenile phase of vegetative growth. *J. Exp. Bot.* **63**, 2787–2798.

Liu, C., Axtell, M.J. and Fedoroff, N.V. (2012) The helicase and RNaseIIIa domains of Arabidopsis Dicer-Like1 modulate catalytic parameters during microRNA biogenesis. *Plant Physiol.* **159**, 748–758.

Llave, C., Xie, Z., Kasschau, K.D. and Carrington, J.C. (2002) Cleavage of Scarecrow-like mRNA targets directed by a class of Arabidopsis miRNA. *Science*, **297**, 2053–2056.

Lobbes, D., Rallapalli, G., Schmidt, D.D., Martin, C. and Clarke, J. (2006) SERRATE: a new player on the plant microRNA scene. *EMBO Rep.* **7**, 1052–1058.

Lu, S. and Cullen, B.R. (2004) Adenovirus VA1 noncoding RNA can inhibit small interfering RNA and MicroRNA biogenesis. *J. Virol.* **78**, 12 868–12 876.

Ma, Z., Hu, X., Cai, W., Huang, W., Zhou, X., Luo, Q., Yang, H., Wang, J. and Huang, J. (2014) Arabidopsis miR171-targeted scarecrow-like proteins bind to GT cis-elements and mediate gibberellin-regulated chlorophyll biosynthesis under light conditions. *Plos Genet.* **10**, e1004519.

Martin, S., Garcia, M.L., Troisi, A., Rubio, L., Legarreta, G., Grau, O., Alioto, D., Moreno, P. and Guerri, J. (2006) Genetic variation of populations of Citrus psorosis virus. *J. Gen. Virol.* **87**, 3097–3102.

Mateos, J.L., Bologna, N.G., Chorostecki, U. and Palatnik, J.F. (2010) Identification of microRNA processing determinants by random mutagenesis of Arabidopsis MIR172a precursor. *Curr. Biol.* **20**, 49–54.

Milne, R.G., García, M.L. and Moreno, P. (2003) Citrus psorosis virus. *Association of Applied Biologists. Descriptions of Plant Viruses*. Available at http://www.dpvweb.net/dpv/showdpv.php?dpvno=401. Date accessed: 18th June, 2015.

Moxon, S., Jing, R., Szittya, G., Schwach, F., Rusholme Pilcher, R.L., Moulton, V. *et al*. (2008) Deep sequencing of tomato short RNAs identifies microRNAs targeting genes involved in fruit ripening. *Genome Res.* **18**, 1602–1609.

Naqvi, A.R., Haq, Q.M. and Mukherjee, S.K. (2010) MicroRNA profiling of tomato leaf curl New Delhi virus (tolcndv) infected tomato leaves indicates that deregulation of mir159/319 and mir172 might be linked with leaf curl disease. *Virol. J.* **7**, 281.

Naum-Ongania, G., Gago-Zachert, S., Pena, E., Grau, O. and Garcia, M.L. (2003) Citrus psorosis virus RNA 1 is of negative polarity and potentially encodes in its complementary strand a 24K protein of unknown function and 280K putative RNA dependent RNA polymerase. *Virus Res.* **96**, 49–61.

Navarro, L., Dunoyer, P., Jay, F., Arnold, B., Dharmasiri, N., Estelle, M., Voinnet, O. and Jones, J.D. (2006) A plant miRNA contributes to antibacterial resistance by repressing auxin signaling. *Science*, **312**, 436–439.

Padmanabhan, M.S., Ma, S., Burch-Smith, T.M., Czymmek, K., Huijser, P. and Dinesh-Kumar, S.P. (2013) Novel positive regulatory role for the SPL6 transcription factor in the N TIR-NB-LRR receptor-mediated plant innate immunity. *Plos Pathog.* **9**, e1003235.

Palatnik, J.F., Allen, E., Wu, X., Schommer, C., Schwab, R., Carrington, J.C. and Weigel, D. (2003) Control of leaf morphogenesis by microRNAs. *Nature*, **425**, 257–263.

Pall, G.S. and Hamilton, A.J. (2008) Improved northern blot method for enhanced detection of small RNA. *Nat. Protoc.* **3**, 1077–1084.

Park, M.Y., Wu, G., Gonzalez-Sulser, A., Vaucheret, H. and Poethig, R.S. (2005) Nuclear processing and export of microRNAs in Arabidopsis. *Proc. Natl. Acad. Sci. USA*, **102**, 3691–3696.

Park, W., Li, J., Song, R., Messing, J. and Chen, X. (2002) CARPEL FACTORY, a Dicer homolog, and HEN1, a novel protein, act in microRNA metabolism in Arabidopsis thaliana. *Curr. Biol.* **12**, 1484–1495.

Pena, E.J., Robles Luna, G., Zanek, M.C., Borniego, M.B., Reyes, C.A., Heinlein, M. and Garcia, M.L. (2012) Citrus psorosis and Mirafiori lettuce big-vein ophiovirus coat proteins localize to the cytoplasm and self interact in vivo. *Virus Res.* **170**, 34–43.

Pfeffer, S. and Voinnet, O. (2006) Viruses, microRNAs and cancer. *Oncogene*, **25**, 6211–6219.

Reyes, C.A., Pena, E.J., Zanek, M.C., Sanchez, D.V., Grau, O. and Garcia, M.L. (2009) Differential resistance to Citrus psorosis virus in transgenic *Nicotiana benthamiana* plants expressing hairpin RNA derived from the coat protein and 54K protein genes. *Plant Cell Rep.* **28**, 1817–1825.

Robles Luna, G., Pena, E.J., Borniego, M.B., Heinlein, M. and Garcia, M.L. (2013) Ophioviruses CPsV and MiLBVV movement protein is encoded in RNA 2 and interacts with the coat protein. *Virology*, **441**, 152–161.

Roistacher, C.N. and **International Organization of Citrus Virologists. and Food and Agriculture Organization of the United Nations** (1991) *Graft-Transmissible Diseases of Citrus : Handbook for Detection and Diagnosis*. Rome: International Organization of Citrus Virologists: Food and Agriculture Organization of the United Nations.

Ruiz-Ruiz, S., Navarro, B., Gisel, A., Pena, L., Navarro, L., Moreno, P., Di Serio, F. and Flores, R. (2011) Citrus tristeza virus infection induces the accumulation of viral small RNAs (21–24-nt) mapping preferentially at the 3'-terminal region of the genomic RNA and affects the host small RNA profile. *Plant Mol. Biol.* **75**, 607–619.

Sánchez de la Torre, E., Riva, O., Zandomeni, R., Grau, O. and García, M.L. (1998) The top component of citrus psorosis virus contains two ssRNAs, the smaller encodes the coat protein. *Mol. Plant Pathol. On-Line*, Available at http://www.bspp.org.uk/mppol/abstract/1019sanc.htm. Date accessed: 18th June, 2015.

Schwab, R., Palatnik, J.F., Riester, M., Schommer, C., Schmid, M. and Weigel, D. (2005) Specific effects of microRNAs on the plant transcriptome. *Dev. Cell*, **8**, 517–527.

Silhavy, D. and Burgyan, J. (2004) Effects and side-effects of viral RNA silencing suppressors on short RNAs. *Trends Plant Sci.* **9**, 76–83.

Singh, K., Talla, A. and Qiu, W. (2012) Small RNA profiling of virus-infected grapevines: evidence for virus infection-associated and variety-specific miRNAs. *Funct. Integr. Genomics*, **12**, 659–669.

Song, C., Jia, Q., Fang, J., Li, F., Wang, C. and Zhang, Z. (2010a) Computational identification of citrus microRNAs and target analysis in citrus expressed sequence tags. *Plant Biol. (Stuttg.)*, **12**, 927–934.

Song, C., Wang, C., Zhang, C., Korir, N.K., Yu, H., Ma, Z. and Fang, J. (2010b) Deep sequencing discovery of novel and conserved microRNAs in trifoliate orange (*Citrus trifoliata*). *BMC Genomics*, **11**, 431.

Song, L., Han, M.H., Lesicka, J. and Fedoroff, N. (2007) Arabidopsis primary microRNA processing proteins HYL1 and DCL1 define a nuclear body distinct from the Cajal body. *Proc. Natl. Acad. Sci. USA*, **104**, 5437–5442.

Swaminathan, G., Martin-Garcia, J. and Navas-Martin, S. (2013) RNA viruses and microRNAs: challenging discoveries for the 21st century. *Physiol. Genomics*, **45**, 1035–1048.

Tagami, Y., Inaba, N., Kutsuna, N., Kurihara, Y. and Watanabe, Y. (2007) Specific enrichment of miRNAs in *Arabidopsis thaliana* infected with Tobacco mosaic virus. *DNA Res.* **14**, 227–233.

Triboulet, R., Mari, B., Lin, Y.L., Chable-Bessia, C., Bennasser, Y., Lebrigand, K., Cardinaud, B., Maurin, T., Barbry, P., Baillat, V., Reynes, J., Corbeau, P., Jeang, K.T. and Benkirane, M. (2007) Suppression of microRNA-silencing pathway by HIV-1 during virus replication. *Science*, **315**, 1579–1582.

Vazquez, F., Gasciolli, V., Crete, P. and Vaucheret, H. (2004) The nuclear dsRNA binding protein HYL1 is required for microRNA accumulation and plant development, but not posttranscriptional transgene silencing. *Curr. Biol.* **14**, 346–351.

Wang, C., Han, J., Liu, C., Kibet, K.N., Kayesh, E., Shangguan, L., Li, X. and Fang, J. (2012) Identification of microRNAs from Amur grape (*Vitis amurensis* Rupr.) by deep sequencing and analysis of microRNA variations with bioinformatics. *BMC Genomics*, **13**, 122.

Wu, M.F., Tian, Q. and Reed, J.W. (2006) Arabidopsis microRNA167 controls patterns of ARF6 and ARF8 expression, and regulates both female and male reproduction. *Development*, **133**, 4211–4218.

Xie, Z., Allen, E., Fahlgren, N., Calamar, A., Givan, S.A. and Carrington, J.C. (2005) Expression of Arabidopsis MIRNA genes. *Plant Physiol.* **138**, 2145–2154.

Xu, Q., Liu, Y., Zhu, A., Wu, X., Ye, J., Yu, K., Guo, W. and Deng, X. (2010) Discovery and comparative profiling of microRNAs in a sweet orange red-flesh mutant and its wild type. *BMC Genomics*, **11**, 246.

Xu, Q., Chen, L.L., Ruan, X., Chen, D., Zhu, A., Chen, C., Bertrand, D., Jiao, W.B., Hao, B.H., Lyon, M.P., Chen, J., Gao, S., Xing, F., Lan, H., Chang, J.W., Ge, X., Lei, Y., Hu, Q., Miao, Y., Wang, L., Xiao, S., Biswas, M.K., Zeng, W., Guo, F., Cao, H., Yang, X., Xu, X.W., Cheng, Y.J., Xu, J., Liu, J.H., Luo, O.J., Tang, Z., Guo, W.W., Kuang, H., Zhang, H.Y., Roose, M.L., Nagarajan, N., Deng, X.X. and Ruan, Y. (2013) The draft genome of sweet orange (*Citrus sinensis*). *Nat. Genet.* **45**, 59–66.

Yin, X., Wang, J., Cheng, H., Wang, X. and Yu, D. (2013) Detection and evolutionary analysis of soybean miRNAs responsive to soybean mosaic virus. *Planta*, **237**, 1213–1225.

Zanek, M.C., Pena, E., Reyes, C.A., Figueroa, J., Stein, B., Grau, O. and Garcia, M.L. (2006) Detection of Citrus psorosis virus in the northwestern citrus production area of Argentina by using an improved TAS-ELISA. *J. Virol. Methods*, **137**, 245–251.

Zhai, J., Jeong, D.H., De Paoli, E., Park, S., Rosen, B.D., Li, Y., Gonzalez, A.J., Yan, Z., Kitto, S.L., Grusak, M.A., Jackson, S.A., Stacey, G., Cook, D.R., Green, P.J., Sherrier, D.J. and Meyers, B.C. (2011) MicroRNAs as master regulators of the plant NB-LRR defense gene family via the production of phased, trans-acting siRNAs. *Genes Dev.* **25**, 2540–2553.

Zhu, H., Xia, R., Zhao, B., An, Y.Q., Dardick, C.D., Callahan, A.M. and Liu, Z. (2012) Unique expression, processing regulation, and regulatory network of peach (*Prunus persica*) miRNAs. *BMC Plant Biol.* **12**, 149.

Zuker, M. (2003) Mfold web server for nucleic acid folding and hybridization prediction. *Nucleic Acids Res.* **31**, 3406–3415.

AUTHOR-RECOMENDED INTERNET RESOURCES

The National Center for Biotechnology Information website: http://www.ncbi.nlm.nih.gov

miRBase: http://www.mirbase.org/
HarvEST: Citrus: http://harvest.ucr.edu
Citrus Genome database: http://www.citrusgenomedb.org/
http://bti.cornell.edu/research/projects/nicotiana-benthamiana/
The Mfold Web Server: http://www.bioinfo.rpi.edu/applications/mfold/
Food and Agriculture Organization of the United Nations: (FAO statistics), http://faostat.fao.org/default.aspx
GraphPad software: http://www.graphpad.com
ImageJ software: http://imagej.nih.gov/ij/

SUPPORTING INFORMATION

Additional Supporting Information may be found in the online version of this article at the publisher's website:

Fig. S1 Processing model of *Citrus sinensis* miR156 family of precursors. Average for the seven members (*C. sinensis* pre-miR156 *a–g*) is shown. A structured region (upper stem) of a conserved length of around 42 nucleotides with a short loop coincides with the loop-to-base model of processing (Bologna *et al*., 2013b). Structures were predicted based on Mfold (Zuker, 2003). The proximal end of the miRNA/miRNA* duplex was defined as position +1. Matches in each position were considered as 0, whereas bulges and mismatches were considered as 1.

Fig. S2 Detection of pre-miR156 family members. Reverse transcription-polymerase chain reaction (RT-PCR) assays to detect *Citrus sinensis* pre-miR156*a*, *b* and *c*. Ubq, ubiquitin used as internal control. Sizes: Ubq, 193 bp; pre156*a*, 83 bp; pre156*b*, 106 bp; pre156*c*, 136 bp.

Fig. S3 Western blot analysis of transiently expressed 24K or 54K of *Citrus psorosis virus* (CPsV) or co-expression of both (24K/54K) in *Nicotiana benthamiana* plants before (INPUT) and after (IP) RNA immunoprecipitation. The two fractions were analysed using anti-green fluorescent protein (α-GFP) antibodies for the GFP-fused viral proteins (left panels) or anti-red fluorescent protein (α-RFP) antibodies for the RFP control (right panels). Coomassie blue-stained sodium dodecylsulfate-polyacrylamide gel electrophoresis (SDS-PAGE) is shown in the lower panel of the INPUT fraction as a loading control.

Table S1 Oligonucleotides used for probes and primers for miRNA, targets, miRNA precursors and internal controls for detection in *Citrus sinensis* and *Nicotiana benthamiana*.

Table S2 Virus quantification in tissues infected with *Citrus psorosis virus* (CPsV) *90-1-1* or *CPV4* isolate expressing each characteristic symptom (F, flecking symptom; Sh, shock reaction symptom; H, healthy leaves).